Invited Paper

Point spread function engineering in confocal scanning microscopy

Manuel Martínez-Corral*
Department of Optics, University of Valencia, E46100 Burjassot, Spain

ABSTRACT

Confocal scanning microscopes are imaging systems that are mainly featured by their unique depth-discrimination capacity when imaging three-dimensional objects. Along the past few years, our research group has done several attempts to improve their axial resolution by means of the so-called point-spread-function (PSF) engineering method. That is, by designing diffractive elements that properly shape the PSF. Our PSF engineering techniques have been designed to work in the nonparaxial regime and are applied both to bright-field and single-photon fluorescence confocal microscopy, and also to more elaborated architectures like 4Pi confocal microscopy.

Key words: PSF engineering, Confocal microscopy, Nonparaxial regime, 3D resolution

1. INTRODUCTION

The improvement of the performance of optical microscopes has aimed many researches along the last decades. Conventional wide-field microscopes are close to reach their maximum efficiency through the use of the available objectives with numerical apertures (NA) up to 1.4. However, when using this kind of microscopes to image three-dimensional (3D) translucent specimens, there is an important drawback: an image focused at a certain depth in a specimen contains blurred information from the entire one. To overcome this trouble, the use of confocal methods was proposed [1]. Confocal scanning microscopes (CSM's) are imaging systems in which the monochromatic light proceeding from a point source is focused onto a point of a 3D specimen by a high NA objective. Afterwards, the light emitted/reflected by the sample is collected by the same objective, passes through a pinhole located at the center of the conjugate plane, and finally is detected. The 3D image is reconstructed with a computer from the intensity values acquired by 3D scanning the sample. In this symmetrical configuration both the illumination and the collection arms play the same role in the imaging properties. The main feature of confocal microscopes is their uncommon depth-discrimination capacity. This capacity results from the ability of CSM's to reject the light proceeding from parts of the object that are not in focus.

However, as it is well known, due to diffraction the axial resolution of confocal setups is, depending on the NA of the lenses, around three times poorer than its lateral counterpart [2]. This difference between axial and lateral resolution leads to an anisotropic 3D-imaging quality.

Several attempts have been made to reduce the axial extent of the point spread function (PSF) of CSM's, and therefore to reduce the anisotropy of the image. Among them we can cite a very ingenious technique consisting in creating a standing wave by the interference of two opposing wave-fronts, as done in the so-called standing-wave microscopy [3] and in 4Pi-confocal microscopy [4]. Standing-wave microscopy is a nonconfocal imaging technique, so that it does not provide any improvement in the depth discrimination capacity. On the contrary, in a 4Pi-confocal microscope two opposing high-NA objectives are used to coherently illuminate and detect the same point of the fluorescence specimen. In case of single-photon fluorescence the resulting PSF has a main peak that is around four times narrower than its lateral counterpart, but that goes with highly enlarged axial sidelobes. Due to these sidelobes the single-photon 4Pi technique does not provide useful images. Nevertheless, by use of two-photon excitation the sidelobes are removed and therefore the technique provides high quality 3D images [5].

An alternative technique to reduce the PSF anisotropy is based on the use of pupil filters. The drawback of using such filters in conventional imaging is that the narrowness of the PSF main peak is obtained at the expense of higher sidelobes. However, in confocal architectures this collateral effect is overcome. Along the past few years several authors have proposed the use of purely absorbing or complex-transmittance pupil filter has been proposed to improve the resolution of confocal microscopes [6,11]. The filters these papers deal with, which are mainly designed to improve the

* manuel.martinez@uv.es; phone +34 96354 4718; fax +34 96354 4715; www.uv.es/imaging3

Wave-Optical Systems Engineering II, Edited by Frank Wyrowski; Proceedings of SPIE
Vol. 5182 (SPIE, Bellingham, WA, 2003) · 0277-786X/03/$15 · doi: 10.1117/12.510209

transverse resolution of confocal microscopes, are inserted in the illumination path, producing then an illumination PSF that is superresolving but with high sidelobes. Due to confocality the sidelobes are strongly reduced in the confocal PSF. Therefore, the implementation of these filters is very useful in bright-field confocal microscopy. However, the filters are less useful in single-photon fluorescence confocal microscopy since the high illumination sidelobes can produce severe photo-bleaching of the specimen at the position of the strong secondary lobes. This does not happen with two-photon fluorescence microscopy. In this case the sidelobes of the illumination PSF are strongly reduced because of the square dependence of the excitation on the illumination intensity, and therefore an effective improvement of resolution is achieved with the using pupil filters [12].

Along the past few years, our research group has addressed important efforts to the design and optimization of new PSF engineering techniques. Our work has been mainly aimed in the improvement of the axial resolution, and therefore the optical-sectioning capacity of confocal setups. In case of single- or two-photon fluorescence microscopy our techniques allows the improvement of axial resolution, but minimizing the increasing of the sidelobes. In other words, they produce an important improvement of the optical sectioning, but minimizing the undesired photo-bleaching effect.

2. THE CONFOCAL POINT SPREAD FUNCTION

Let us start by considering a radially-symmetric confocal scanning imaging system, like the one shown in Fig. 1. Note that, for the sake of plot simplicity, we have drawn a transmission-mode confocal system. In most of real cases the confocal systems work in reflection mode. Thus in this kind of systems, the monochromatic light proceeding from the point source is focused onto a small region of the 3D sample. This region constitutes the object for the collection arm, which collects the light reflected/emitted by the sample and focuses it onto a pinhole. The light passing the pinhole is detected. After this process it is obtained information about only a singular point of the 3D object. The 3D image is reconstructed with a computer from the intensity values acquired by 3D scanning the sample.

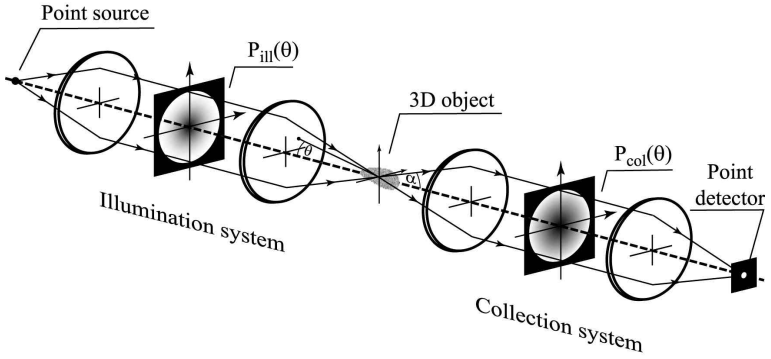

Figure 1. Schematic diagram of a confocal scanning microscope

Depending on the type of confocal system, the intensity distribution of confocal image is given by:

a) Bright field confocal microscopy (the collected light is coherent):

$$I(\mathbf{r}, z; \lambda) = \left| o(\mathbf{r}, z) \otimes_3 psf(r, z; \lambda) \right|^2 \quad , \tag{1}$$

where $o(\mathbf{r}, z)$ represents the amplitude transmittance/reflectance at any point of the 3D object, and

$$psf(r, z; \lambda) = h_{ill}(r, z; \lambda) h_{col}(r, z; \lambda) \tag{2}$$

is the amplitude PSF of the bright-field confocal microscope, which result from the product between the amplitude PSF's of the illumination and the collection arms. λ is the wavelength of the light.

b) Single-photon confocal fluorescence microscopy (in fluorescence imaging the emitted light is incoherent):

$$I(\mathbf{r}, z; \lambda_{ill}, \varepsilon) = O(\mathbf{r}, z) \otimes_3 PSF(r, z; \lambda_{ill}, \varepsilon) \quad , \tag{3}$$

where $O(\mathbf{r}, z)$ is the 3D function that describes the spatial distribution of the fluorescence generation, and

$$PSF(r,z;\lambda_{ill},\varepsilon)=\left|h_{ill}(r,z;\lambda_{ill})\right|^2\left|h_{col}(r,z;\lambda_{ill}/\varepsilon)\right|^2 \tag{4}$$

is the intensity PSF of the incoherent imaging system. Parameter $\varepsilon=\lambda_{ill}/\lambda_{col}$ accounts for the ratio between the excitation and the fluorescence wavelengths.

Since confocal microscopes incorporate objectives with high numerical aperture, the function $h(r,z;\lambda)$, which represents the nonparaxial amplitude PSF of a focusing lens, is given within the scalar Debye diffraction theory [13], by

$$h(r,z)=\int_0^{\alpha}\mathrm{P}(\theta)\,\mathrm{J}_0(k\,r\sin\theta)\exp(-ikz\cos\theta)\sin\theta\,d\theta\ , \tag{5}$$

where $k=2\pi n/\lambda$. In Eq. (5), which is a Bessel transform over the aperture angle θ, function $\mathrm{P}(\theta)$ accounts for the amplitude transmittance at the aperture stop, and α is the maximum value of the aperture angle.

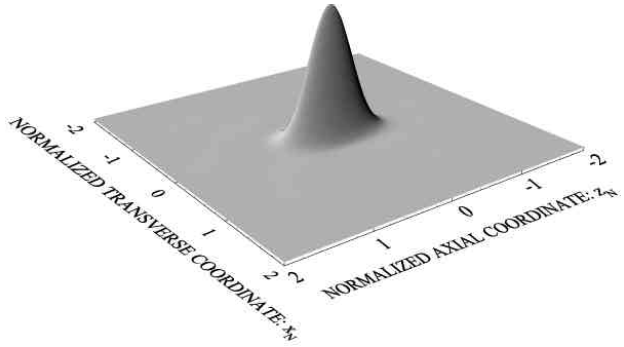

Figure 2. Meridian section of the three-dimensional intensity PSF of a bright-field confocal scanning microscope. The normalized coordinates are $z_N=n(1-\cos\alpha)z/\lambda$ and $x_N=(n/\lambda)x\sin^2\alpha$.

The most important feature of, both bright-field and fluorescence, confocal microscopes is their proverbial depth discrimination capacity. This capacity proceeds from the ability of the pinholed detection to reject light proceeding from points of the sample not of focus. However, even for the highest value of the NA, the axial extent of the PSF is at least three times bigger that the lateral counterpart (see Fig. 2). This difference leads to an anisotropic 3D imaging quality, because the axial details are worse resolved than the transverse details. Then the search for techniques that allow to compress the axial PSF, and therefore to reduce the anisotropy of confocal microscopes, is a matter of especial interest. To tackle such a task is convenient starting with the analysis of the axial PSF. To this end we set $r=0$ in Eq. (5) and perform the nonlinear mapping

$$\zeta=\frac{\cos\theta-\cos\alpha}{1-\cos\alpha}-0.5\quad;\qquad Q(\zeta)=P(\theta)\ , \tag{6}$$

to obtain

$$h(z_N)=(1-\cos\alpha)\exp\left(i\pi\frac{1+\cos\alpha}{1-\cos\alpha}\,z_N\right)\int_{-0.5}^{0.5}Q(\zeta)\exp(i2\pi\zeta z_N)\mathrm{d}\zeta\ , \tag{7}$$

where $z_N=n(1-\cos\alpha)z/\lambda$. Eq. (7) indicates that the axial amplitude PSF of a lens is proportional to the 1D Fourier transform of the nonlinearly mapped transmittance $Q(\zeta)$. If the aperture of the lens is circular, then $Q(\zeta)$ is a rectangle. In that case the calculation of the intensity PSF of confocal arrangements is very simple: is proportional to $\mathrm{sinc}^4(z_N)$ in a bright-field confocal microscope, and to $\mathrm{sinc}^2(z_N)\mathrm{sinc}^2(\varepsilon z_N)$ in a single-photon fluorescence confocal microscope.

3. PSF ENGINEERING IN CONFOCAL MICROSCOPY

To properly tailor the axial PSF of confocal microscopes by means of PSF engineering, it is necessary to investigate for a function $Q(\zeta)$ whose 1D Fourier transform closely approximates the desired form for the PSF of the illumination arm. Take into account that due to the pinhole, the light efficiency of confocal detection is very low, and therefore any mask should be inserted in the illumination arm, to avoid light losses in detection. We have developed different PSF engineering techniques for the improvement of the optical sectioning capacity of confocal microscopes.

In a first attempt we designed binary filters for achieving axial resolution [14]. To obtain axial resolution, the standard deviation of the mapped transmittance of the filter must be greater than the one of the clear circular aperture. Therefore we designed a set of binary filters such that their mapped functions consist of two equal-width rectangles. Note that the smaller the width of the rectangles the higher the axial gain in resolution but the higher the sidelobes height as well. The actual 2D form of the filter consist in a dark ring centered in the circular aperture. Therefore this kind of filters will be named hereafter as the dark ring (DR) filters. The selection the optimum filter is the result of a trade off. We found that the axial resolution of a bright-field confocal microscope can be improved up to a 30%, as shown in Fig. 3.

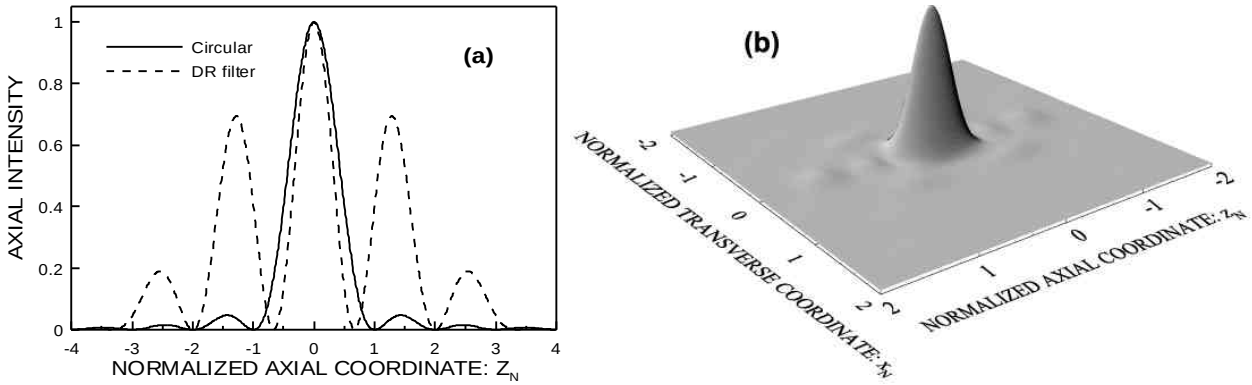

Figure 3. (a) Axial PSF of the DR filter as compared with the one of the circular aperture. If a bright-field confocal microscope incorporates a DR filter in illumination and a circular aperture in collection, the axial-confocal PSF results from the product of these two curves. (b) Meridian section of the three-dimensional intensity PSF of a bright-field confocal scanning microscope that incorporates the DR filter in illumination. Compare with the plot in Fig. 2.

The aim of narrowing the central lobe of the illumination PSF of a bright-field confocal microscope can be achieved more efficiently by use of phase-only filters. In this sense, Toraldo di Francia [15] showed that the radii of the zero-intensity rings in the focal plane of a paraxial focusing system can be selected at will by using a pupil filters subdivided into concentric zones with constant transmittance. We have adapted the Toraldo concept to a new situation: the control of the shape of the axial PSF of non-paraxially focusing systems. We therefore outline the similarities and differences between the original Toraldo algorithm and our procedure. In the original algorithm the amplitude transmittance of the filter, $t(r)$, is subdivided into m concentric annular zones to control the radii of $m-1$ rings of zero intensity. In our approach the function $Q(\zeta)$ is also subdivided into constant-transmittance zones [16]. Here it is important to take into account that if one wants to tailor the axial PSF with the constraint that the transverse PSF should remain almost invariant, the resulting function $Q(\zeta)$ must be centro-symmetric. This implies that to control the positions of $m-1$ axial zeros, the interval [-0.5, 0.5] should be divided into $2m-1$ subintervals such that in each subinterval the function $Q(\zeta)$ is constant. On the basis of the above reasoning we designed the Toraldo filter shown in Fig. 4. The filter is composed by seven rings, having each pair of neighboring rings opposite phases. This filters permits to control the position of three axial zeros. The first one is used to determine the extent of the central lobe. The other two are used to send far away the huge sidelobe inherent to Toraldo filtering. Note from Fig. 5 that the Toraldo technique allows the improvement of confocal axial resolution and that the sidelobes in the confocal PSF almost vanished.

Note that the, purely-absorbing or phase-only, proposed filters are inserted in the illumination path, producing then an illumination PSF that is axially superresolving but with high sidelobes. Due to confocality the sidelobes are strongly reduced in the confocal PSF. Therefore, these filters are very useful in bright-field confocal microscopy, and have potential application in fields like ophthalmology of profilometry. However, the filters are less useful in single-photon

fluorescence confocal microscopy since the high illumination sidelobes can produce severe photo-bleaching of the specimen at the position of the strong secondary lobes. Then the design constraints of the filters should include the control of the sidelobes height.

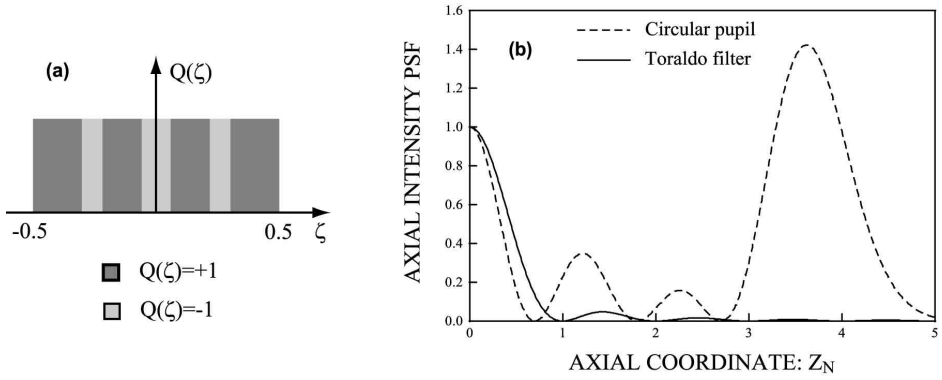

Figure 4. (a) Mapped transmittance of the seven-zone Toraldo filter, which allows the control of positions of three axial zeros; (b) Axial PSF of the Toraldo filter as compared with the one of the circular aperture. If a bright-field confocal microscope incorporates a Toraldo filter in illumination and a circular aperture in collection, the axial-confocal PSF results from the product of these two curves. Note that the huge sidelobe has been sent to a point where the collection PSF is very low.

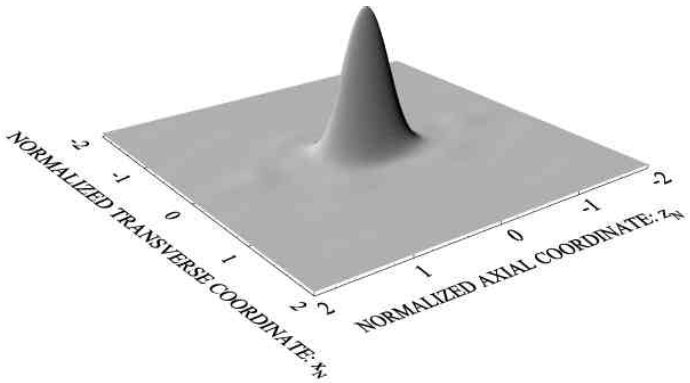

Figure 5. Meridian section of the three-dimensional intensity PSF of a bright-field confocal scanning microscope that incorporates the Toraldo filter in illumination and a circular aperture in collection. If we compare with Fig. 4b, we find that the same narrowness of the central lobe is obtained, but now the sidelobes are much lower.

In our first attempt of designing masks for application in confocal fluorescence microscopy, we have adapted the Boyer's [17] concept to the optical axis, and have designed a new type of annular binary filters [18]. In this new design we simply add to the DR filters a new transparent ring centered at $\zeta = 0$. Note that these new filters, known as three-ring (3R) filters, reproduce in certain way the Young experiment but along the optical axis. In terms of this experiment it is easy to understand the axial behavior of the filters. The inner and the outer rings produce an axial pattern with narrow central lobe but high sidelobes (like in a Young experiment with finite-width slits). The central ring mainly contributes to the height of the central lobe. The combination of both effects results in an axial pattern with a narrow main peak and low sidelobes. After a comprehensive process of optimization we selected the filter shown in Fig. 6. In our numerical experiment we inserted the filter in the illumination path of a confocal fluorescence microscope, schematized in Fig. 6 as well. In this scheme the relay lenses are used to focus the filter into the front focal plane of the objective. We calculated the 3D PSF corresponding to the illumination, the collection, and the confocal system (see Fig. 7). The parameters for the calculations were $\lambda_{ill} = 350\ nm$, $\varepsilon = 0.8$, NA=1.4 (oil). After comparing these figures with the ones of the non-apodized setup (not shown) we found an important improvement (11.3% in terms of the HMW) of two-point axial resolution, which is obtained after a moderate increase of the illumination sidelobes. Besides, the lateral confocal PSF obtained with the 3R filter is only a 0.7% wider (in terms of the HMW) than the PSF obtained without the filter. Therefore, it can be stated that the use of 3R filters hardly affects to the transverse resolution.

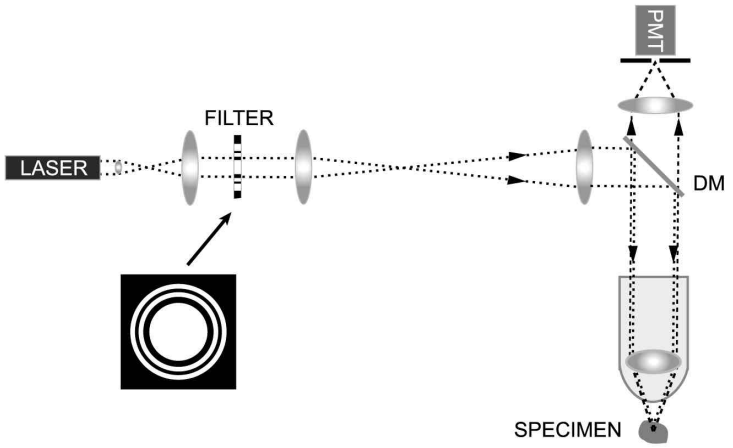

Figure 6. Schematic geometry of a single-photon, fluorescence confocal microscope. The selected 3R filter is inserted in the illumination arm. Relay lenses are used to focus the 3R filter into the back focal plane of the objective.

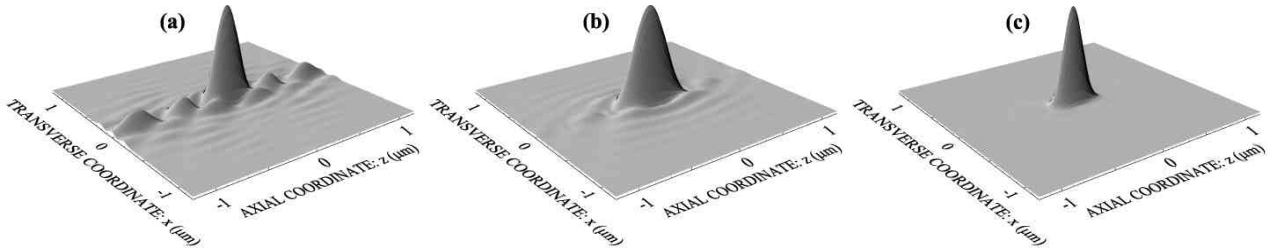

Figure 7. Plots of the 3D PSF, in meridian the plane, corresponding to: (a) Illumination arm with the 3R filter; (b) Detection arm; (c) Confocal system.

A second approach to the problem of PSF engineering in confocal fluorescence microscopy is the use of the so-called shaded-ring (SR) filters [19]. The SR filters consist of a single shaded ring centered on a circular pupil, and have the ability of tuning the width of axial spot main peak, but attenuating the sidelobe energy. The performance of SR filters, as compared with the DR filters, is illustrated in Fig. 8. Note that the contribution of the shaded ring to the axial pattern is significant only in the central part. Then, the axial intensity produced by the SR filter (bold curve in Fig 8b) exhibits a central lobe that is much higher than the one produced by the DR filter (dashed curve in Fig. 8b), whereas the sidelobes height remains almost invariant. The SR filters can be understood as members of a more general class of filters known as leaky filters. Besides, it can be shown that given a value for the axial gain in resolution it can be built a whole family of SR filters with tunable sidelobes energy.

The selection of the optimum filter is application dependent. For application in single-photon fluorescence confocal microscopy, we will select, among the family of SR filters with the same axial gain, the filter that minimizes the sidelobes to peak ratio (SLPR), defined as

$$SLPR = \int_{z_p}^{+\infty} \left|\mathrm{h}_{ill}(r=0, z:\lambda_{ill})\right|^2 dz \Big/ \int_{0}^{z_p} \left|\mathrm{h}_{ill}(r=0, z;\lambda_{ill})\right|^2 dz \quad , \tag{8}$$

z_p being the coordinate of the first zero-intensity axial point. In Fig. 9a we have drawn several curves with constant value for axial gain G_A (defined as the ratio between the half-maximum width (HMW) of the axial PSF obtained with the circular aperture and the one obtained with the SR filter) but varying *SLPR*. Any point at the curves corresponds to a different SR filter. The point at the left end of each curve corresponds to the DR filter (which now is considered as a member of the SR-filters family). For our numerical experiment we selected an axial gain of 20%. The minimum of the curve corresponds to the SR filter m=0.67 and h=0.66. Note that the *SLPR* of the selected filter is 25% better than the one of the DR filter. We also show the 3D PSF of a confocal instrument with two circular pupils (Fig. 9b) and with the SR filter in the illumination and the circular pupil in collection (Fig. 9c). It is obtained an important improvement (12.0% in terms of the HMW) in axial resolution, and only a small worsening (1.8%) in lateral resolution.

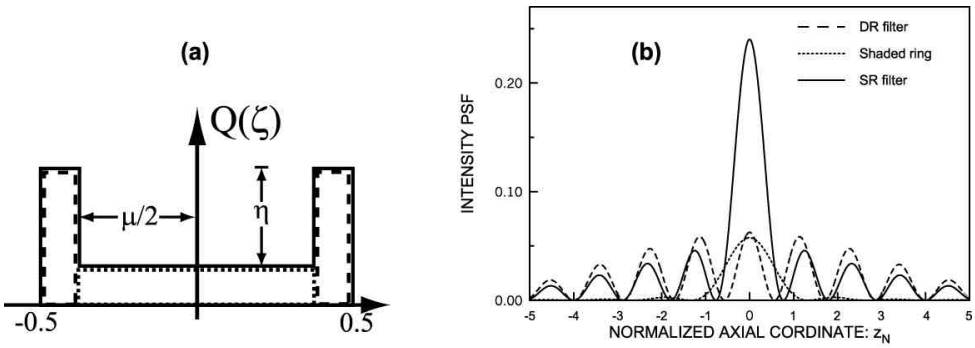

Figure 8. (a) Mapped transmittance of a SR filter (bold curve). The SR filter can be understood as composed by a DR filter (dashed curve) and a shaded ring (dotted curve); (b) Intensity axial PSF of the SR filter (bold curve). The amplitude PSF of the SR filter can be calculated as the sum of two amplitude PSF's: the corresponding to the DR filter and that of the shaded ring.

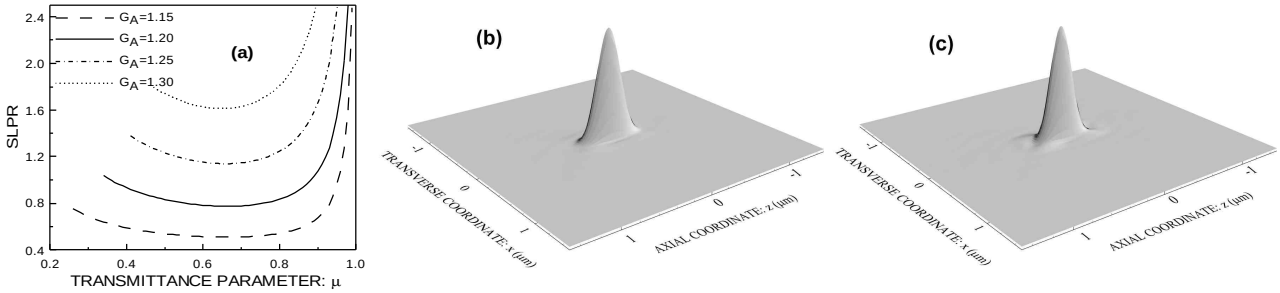

Figure 9. (a) *SLPR* values for families of SR filters with the same axial gain; (b) numerically evaluated 3D PSF of a confocal instrument with two circular pupils; (c) same as (b) but with the selected SR filter in illumination. The parameters for the calculation where: l_{ill}=350 nm, e=0.8 and NA=1.2 (water).

The optical-sectioning capacity of an imaging system is better evaluated in terms of the so-called *z*-response, which is defined as the 1D image acquired by axially scanning a very thin fluorescent layer. In Fig. 10 we plot the *z*-response for both cases: with and without the SR filter. The SR filter narrows the *z*-response by 12.5%. The same narrowness would be obtained by using an objective with circular aperture and $NA = 1.246$.

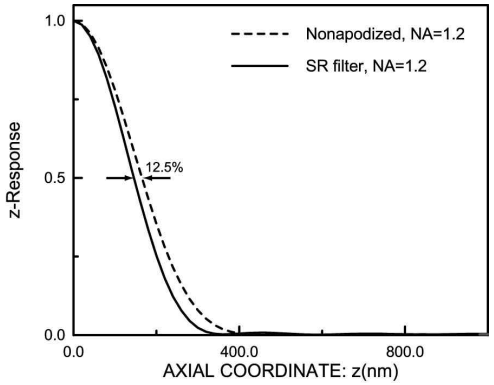

Figure 10. z-responses of the confocal setups under study.

4. NONCONVENTIONAL CONFOCAL MICROSCOPES

PSF engineering techniques can also be applied to improve the performance of more complex confocal architectures like the so-called 4Pi confocal microscopes [4]. In these systems the 3D specimen is illuminated by the standing wave generated by the interference between the two opposing, tightly focused waves proceeding from the high NA objectives. The light emitted by the fluorescent specimen is collected by the same objectives, and interfere at the pinhole plane (see Fig. 11).

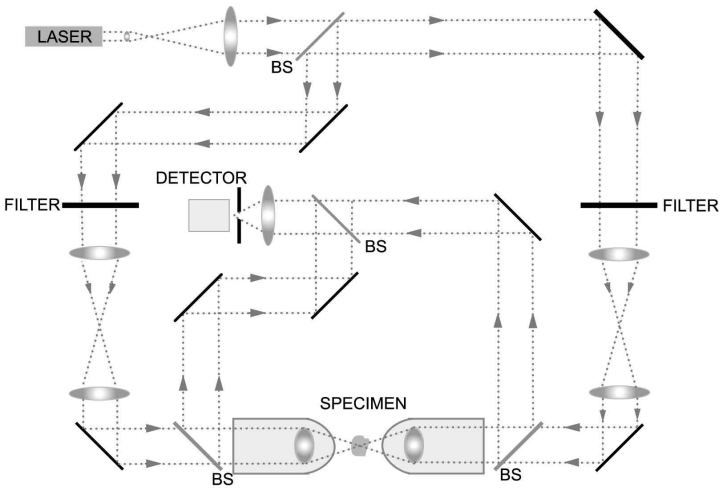

Figure 11. Schematic geometry of a 4Pi apodized confocal microscope. Relay lenses are used to focus the pupil filters into the back focal plane of the objectives.

The 3D PSF of 4Pi confocal microscopes is given by

$$PSF_{4\mathrm{Pi}}(z,r;\lambda_{ill},\varepsilon)=\left|\mathrm{h}_{ill}(r,z;\lambda_{ill})+\mathrm{h}_{ill}(r,-z;\lambda_{ill})\right|^2\left|\mathrm{h}_{col}(r,z;\varepsilon\lambda_{ill})+\mathrm{h}_{col}(r,-z;\varepsilon\lambda_{ill})\right|^2. \tag{9}$$

To analyze the axial behavior of 4Pi microscopes we set $r=0$, substitute Eq. (7) into Eq. (9), and obtain

$$PSF_{4Pi}(z_N)=4(1-\cos\alpha)^2\left|\cos\left(\pi\frac{1+\cos\alpha}{1-\cos\alpha}z_N\right)\tilde{Q}(\zeta)\right|^2\left|\cos\left(\pi\frac{1+\cos\alpha}{1-\cos\alpha}\varepsilon z_N\right)\tilde{Q}(\varepsilon\zeta)\right|^2, \tag{10}$$

where $\tilde{Q}$ represents the 1D Fourier transform of function Q. From the above equation is clear that the illumination PSF is given by the product between a $\cos^2$ factor (the standing wave factor) and function $\tilde{Q}^2$ (the modulating factor), which in case of circular apertures is proportional to $\mathrm{sinc}^2(z_N)$. The collection PSF is the same but scaled by ε.

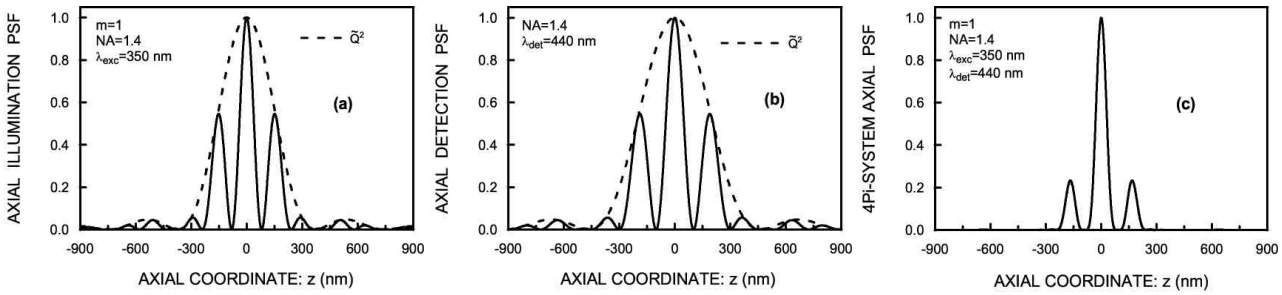

Figure 12 Numerically evaluated axial intensity PSF corresponding to: (a) Illumination system in case of single-photon absorption; (b) Detection system (dashed curves correspond to the enveloping function); and (c) Single-photon 4Pi-confocal microscope.

An example of axial PSF is shown in Fig. 12, where we selected for the calculations the highest allowable NA. In the example we set $n = 1.518$, $\alpha = 67.5$ (NA=1.4), $\lambda_{ill} = 350\,nm$ and $\varepsilon = 0.8$. Note that illumination (Fig. 12a) and detection (Fig. 12b) axial PSFs exhibit a very narrow central lobe, but high axial sidelobes. The 4Pi-system PSF is obtained after multiplying the curves in Figs. 12a and 12b. The resulting curve has a central lobe whose width is imposed by the one of the illumination-PSF core. Due to the multiplicative process the sidelobes height has downed to 23% of the main peak. However, the sidelobes are still too high and they can produce artifacts in the 3D image.

To overcome theses problems we propose is the use of annular, purely-absorbing [20] or phase-only[21], pupil masks in one-photon 4Pi-confocal microscopy to reduce the strength of the PSF axial sidelobes. The cornerstone of our method is to design pupil filters with the ability of compressing the illumination axial PSF so that in the confocal-multiplicative process the secondary peak of the illumination axial PSF is multiplied by low values of the detection axial PSF, and vice-versa. In other words, we propose the use of axially superresolving pupil filters, which in conventional imaging produce high axial sidelobes, to paradoxically obtain an apodization effect in 4Pi-confocal microscopy, i.e. a severe reduction of axial sidelobes. The filters we propose to use are similar to the DR filters or to the Toraldo filters described above. To illustrate the utility of the technique, next in Fig. 13 we compare two different PSFs: the corresponding to a 4Pi microscope with a properly designed seven-zone Toraldo filters in the illumination arm, and the one of a 4Pi microscope without filters. Note that the highest sidelobe has been downed to 7% of the main peak, which is 3.3 times lower than the one obtained without the Toraldo filter.

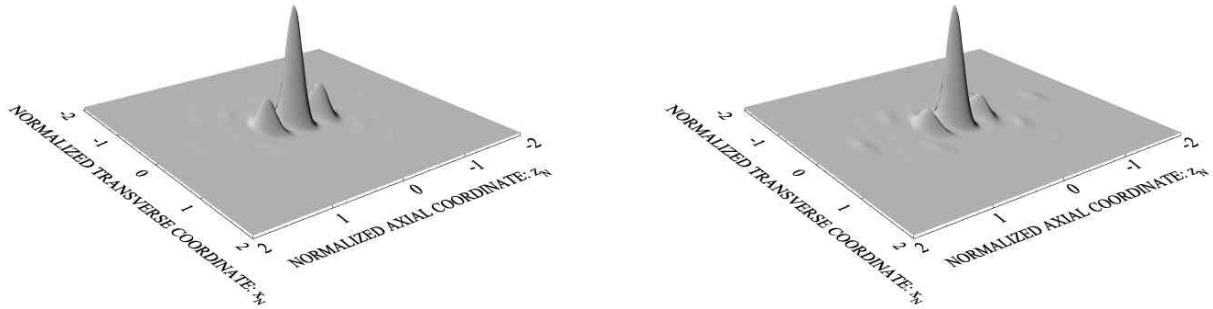

Figure 13. (a) numerically evaluated 3D PSF of a 4Pi confocal instrument with two circular pupils; (b) same as (a) but with the selected seven-zone Toraldo filter in illumination. The parameters for the calculation where: l_{ill}=350 nm, e=0.8 and NA=1.4 (oil).

To complete the study of PSF engineering in 4Pi confocal microscopy, we carried out a numerical experiment, by calculating the resulting 3D image of a test object. We designed an elaborated 3D object consisting of two concentric spherical fluorescence labeled shells, as shown in Fig 14a. The test object was designed to contain all the axial and transverse frequencies of interest. The dark band in the object will permit us to clearly visualize the improvement in resolution along the different directions passing through the focus. After convolution with the confocal PSF (see Fig. 2) and with the Toraldo 4Pi PSF (represented in Fig 13b), we obtained the simulated images shown in Fig. 14b-c. Note that no worsening in the transverse direction is achieved. Concerning the axial direction, the amount of blur in the image of the test-object dark band (devoid of fluorescence) is significantly lower in case of Toraldo 4Pi setup.

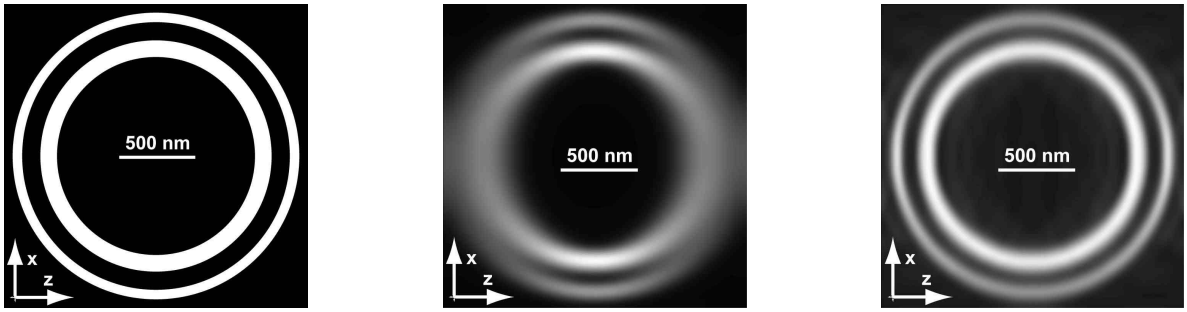

Figure 14. Imaging of the elaborated 3D object. (a) Test object consisting of two concentric spherical fluorescence labeled shells; (b) Axial section of the calculated image for the case of the confocal microscope; (c) same as (b) but for the 4Pi confocal microscope with the Toraldo filter in illumination.

5. CONCLUSIONS

We have shown that the PSF engineering techniques can be very useful to improve the performance of modern 3D imaging systems. Specifically we have designed different families of radially symmetric pupil filters for application in bright confocal microscopy, fluorescence confocal microscopy or 4Pi microscopy. In any the designing procedure has been adapted to the specific features of the technique. The PSF engineering techniques have also potential application in multi-photon microscopy.

ACKNOWLEDGEMENTS

This work has been funded by the Plan Nacional I+D+I (Grant DPI2000-0774), Ministerio de Ciencia y Tecnología, Spain.

REFERENCES

1. T. Wilson (ed), *Confocal Microscopy*, Academic, London, 1990.
2. J. Pawley (ed), *Handbook of Biological Confocal Microscopy*, Plenum, New York, 1995.
3. B. Bailey, D. L. Farkas, D. Lansing-Taylor and F. Lanni, "Enhancement resolution in fluorescence microscopy by standing-wave excitation," Science **366**, 44-48 (1993).
4. M. Nagorni and S. Hell, "Coherent use of opposing lenses for axial resolution increase in fluorescence microscopy. I. Comparative study of concepts," J. Opt. Soc. Am. A **18**, 36-48 (2001).
5. C. M. Blanca, J. Bewersdorf and S. W. Hell, "Single sharp spot in fluorescence microscopy of two opposing lenses," Appl. Phys. Lett. **79**, 2321-2323 (2001).
6. M. A. A. Neil, R. Juskaitis, T. Wilson, Z. J. Laczik and V. Sarafis, "Optimized pupil-plane filters for confocal microscope point-spread function engineering," Opt. Lett. **25**, 245-247 (2000).
7. Z. Ding, G. Wang, M. Gu, Z. Wang and Z. Fan, "Superresolution with an apodization film in a confocal setup," Appl. Opt. **36**, 360-363 (1997).
8. M. Kowalczyk, C. J. Zapata-Rodríguez and M. Martínez-Corral, "Asymmetric apodization in confocal imaging systems," Appl. Opt. **37**, 8206-8214 (1998).
9. C. J. R. Sheppard, "Binary optics and confocal imaging," Opt. Lett. **24**, 505-506 (1999).
10. C. M. Blanca and S. W. Hell, "Sharp spherical focal spot by dark ring 4Pi-confocal microscopy," Single Molecules **2**, 207-210 (2001).
11. G. Boyer and V. Sarafis, "Two pinhole superresolution using spatial filters," Optik **112**, 177-179 (2001).
12. C. M. Blanca and S. W. Hell, "Axial superresolution with ultrahigh aperture lenses," Opt. Express **10**, 893-898 (2002)
13. M. Gu, *Advanced optical imaging theory*, Springer-Verlag, Berlin, 2000.
14. M. Martínez-Corral, P. Andrés, C. J. Zapata-Rodríguez and M. Kowalczyk, "Three-dimensional superresolution by annular binary filters," Opt. Commun. **165**, 267-278 (1999).
15. G. Toraldo di Francia, "Nuovo pupille superresolventi," Atti Fond. Giorgio Ronchi **7**, 366-372 (1952).
16. M. Martínez-Corral, M. T. Caballero, E. H. K. Stelzer and J. Swoger, "Tailoring the axial shape of the point spread function using the Toraldo concept," Opt. Express **10**, 98-103 (2002).
17. G. R. Boyer, "Realisation d'un filtrage super-résolvant," Opt. Acta **30**, 807-816 (1983).
18. M. Martínez-Corral, C. Ibáñez-López, M. T. Caballero, L. Muñoz-Escrivá and G. Saavedra, "Three-ring filters increase the effective NA up to 1.46 in optical sectioning fluorescence microscopy", J. Phys. D: Appl. Phys. **36**, 1669-1674 (2003).
19. M. Martínez-Corral, C. Ibáñez-López, G. Saavedra and M. T. Caballero, "Axial gain in resolution in optical-sectioning fluorescence microscopy by shaded-ring filters", Opt. Express **11**, 1740-1745 (2003).

20. M. Martínez-Corral, A. Pons and M. T. Caballero, “Axial apodization in 4Pi-confocal microscopy by annular binary filters”, J. Opt. Soc. Am. A **19**, 1532-1536 (2001).
21. M. Martínez-Corral, M. T. Caballero, A. Pons and P. Andrés, “Sidelobe decline in single-photon 4Pi microscopy by Toraldo rings”, Micron **34**, 319-325 (2003).